

# Boosting WiFi Sensing Performance via CSI Ratio

Youwei Zeng  and Dan Wu , Peking University, Beijing 100871, China

Jie Xiong , University of Massachusetts Amherst, Amherst 01003, USA

Daqing Zhang, Peking University Telecom SudParis, Beijing 100871, China

*The past few years have witnessed the great potential of exploiting channel state information (CSI) retrieved from commodity WiFi devices for contactless human sensing. However, a severe problem hindering practical WiFi sensing applications is that the obtained CSI data contains a large amount of noise, leading to short sensing range and low sensing accuracy. Aiming at solving the critical problem, in this article, we propose to employ a new base signal called CSI ratio to boost the WiFi sensing performance.*

With the rapid progress of wireless technologies, WiFi and cellular networks have been pervasively deployed in our surrounding environments, enabling always-on connection to the Internet. Traditionally, WiFi is only utilized for data communication. It can now be creatively used for human sensing in a nonintrusive manner.

The key enabler for such contactless WiFi human sensing is the channel state information (CSI) retrieved from WiFi devices, which characterizes how the wireless signals propagate from the transmitter to the receiver<sup>1</sup>. In a typical sensing scenario, the WiFi transmitter and receiver are installed separately. When a person conducts a daily activity, the movements of his/her body cause changes in the wireless signal reflections, which lead to variations in CSI. Those variations in CSI could be linked to corresponding human activities by mathematical models,<sup>2,3</sup> which could be further employed to infer rich context information about the person. With this idea, a lot of human sensing applications could be enabled, ranging from activity recognition and indoor localization to vital sign monitoring.

Though promising, due to the physical separation between the transmitter and receiver, the synchronization error between them is introduced, which randomly affects CSI phase and makes it unusable for human sensing in practice.<sup>4,5</sup> Fortunately, its impact on CSI

amplitude is marginal. As a consequence, lots of existing WiFi-based sensing approaches<sup>2,3,6,7</sup> employ only the coarse CSI amplitude readings for sensing. However, such usage leads to two critical limitations. One is the limited sensing range. The existing approaches work poorly or even completely fail when the target is several meters away from the sensing WiFi devices, which restricts the potential applications. The other is the limited sensing accuracy. Most existing approaches only work in fixed or controlled environmental settings.<sup>8,9</sup> And when the target conducts activities in different locations relative to the transceivers, the sensing accuracy varies greatly.<sup>10</sup>

In this article, we propose to employ a new base signal called CSI ratio to overcome the above two limitations. The CSI ratio refers to the quotient of the CSI readings from two adjacent antennas at the same receiver. Leveraging multi-in multi-out (MIMO) technologies, the CSI ratio possesses orthogonal and complementary amplitude/phase information with high signal-to-noise ratio (SNR), enabling longer sensing range and higher sensing accuracy. In addition, the proposed CSI ratio is also applicable to other wireless signals such as the OFDM (Orthogonal Frequency Division Multiplexing)-based LTE (Long Term Evolution) signal<sup>11</sup> and the chirp-modulated LoRa signal<sup>12</sup> for human sensing.

## BACKGROUND AND CHALLENGES

### CSI Primer

WiFi CSI describes how the OFDM signals get attenuated, faded, and scattered by surrounding objects during propagation.<sup>1</sup> For a pair of commodity WiFi

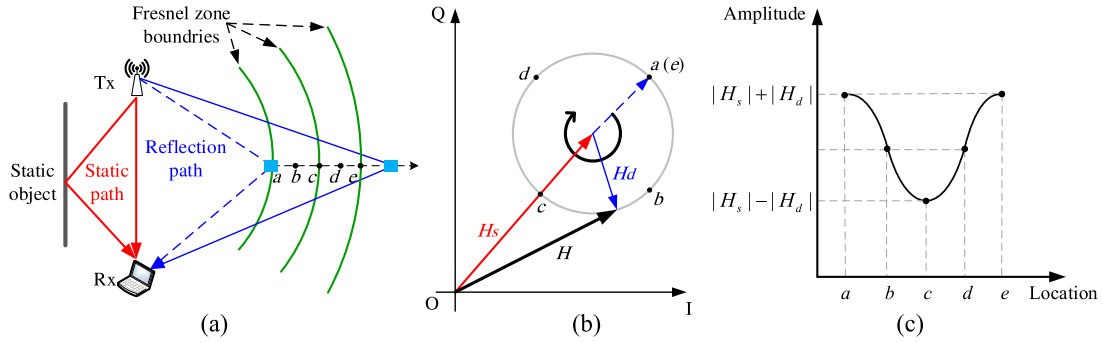


**FIGURE 1.** Illustration of the relationship between target movements and CSI amplitude variations. (a) Target moves from location a to location e. (b) Phasor representation of ideal CSI, which is composed of the static component  $H_s$  and the dynamic component  $H_d$ . (c) CSI amplitude with respect to different target locations.

devices, the measured CSI is affected not only by the signal propagation paths between transceivers but also the hardware imperfection.<sup>1</sup> On the one hand, the power amplifier uncertainty in RF chain often results in impulse and burst noise in CSI amplitude.<sup>13</sup> On the other hand, the difference in carrier frequencies between transceivers leads to a time-varying phase offset in each CSI sample,<sup>14,15</sup> which accumulates quickly over time and messes up the phase variation caused by human movement. Mathematically, the CSI obtained from commodity WiFi can be denoted as

$$H(f, t) = \delta(t)e^{-j\phi(t)} \sum_{l=1}^L A_l(t)e^{-j2\pi\frac{d_l(t)}{\lambda}} \quad (1)$$

where  $\delta(t)$  is the amplitude impulse noise,  $\phi(t)$  is the time-varying phase offset,  $L$  is the total number of propagation paths,  $\lambda$  is the wavelength,  $A_l(t)$  and  $d_l(t)$  are the signal attenuation and length of the  $l$ th path, respectively.

### Human Sensing With WiFi CSI

Figure 1(a) presents a typical contactless sensing system setup, where a WiFi transceiver pair is placed at fixed locations and a target moves away with respect to the transceivers. We introduce the Fresnel zone model<sup>3,7</sup> to illustrate how a moving target affects the WiFi CSI in this scenario. We can see from Figure 1(a) that the propagation paths can be grouped into static path and dynamic path. The static path consists of the line-of-sight (LoS) propagation between transceivers and the reflection paths from static objects in surrounding environment. And the dynamic path is the path reflected from the moving target. When the target moves a short distance, the signal attenuation of the dynamic path can be considered as a

constant.<sup>5,7</sup> This is because the signal attenuation is determined by the path length. Changes of a few centimeters in path length have very little effect when the path length is in the scale of meters. Therefore, the CSI in (1) can be simplified as follows:

$$\begin{aligned} H(f, t) &= \delta(t)e^{-j\phi(t)}(H_s + H_d(f, t)) \\ &= \delta(t)e^{-j\phi(t)}(H_s + Ae^{-j2\pi\frac{d(t)}{\lambda}}) \end{aligned} \quad (2)$$

where  $H_s$  is the static component corresponding to the static path and  $H_d(f, t)$  is the dynamic component corresponding to the dynamic path. Figure 1(b) presents the phasor representation of the ideal CSI, where there is no amplitude impulse noise  $\delta(t)$  and time-varying phase offset  $\phi(t)$ . As shown in Figure 1, when the target moves from a to e, the target-reflection path length increases and the dynamic phasor component of the ideal CSI rotates clockwise in complex plane accordingly.

And the CSI amplitude is the magnitude of the complex CSI data  $H(f, t)$

$$|H(f, t)| = \delta(t) \sqrt{|H_s|^2 + |H_d|^2 + 2|H_s||H_d|\cos\rho} \quad (3)$$

where  $\rho$  is the phase difference between the dynamic component and the static component. As shown in Figure 1(c), when the target crosses a series of Fresnel zone boundaries, the CSI amplitude shows a continuous sinusoidal-like waveform, with peaks and valleys generated by crossing the boundaries. When the reflection path length changes less than one wavelength, the dynamic vector rotates for less than one cycle and the CSI amplitude is just a fragment of the sinusoidal-like waveform, and its shape depends on the target's moving trajectory with respect to the transceivers.<sup>4</sup>

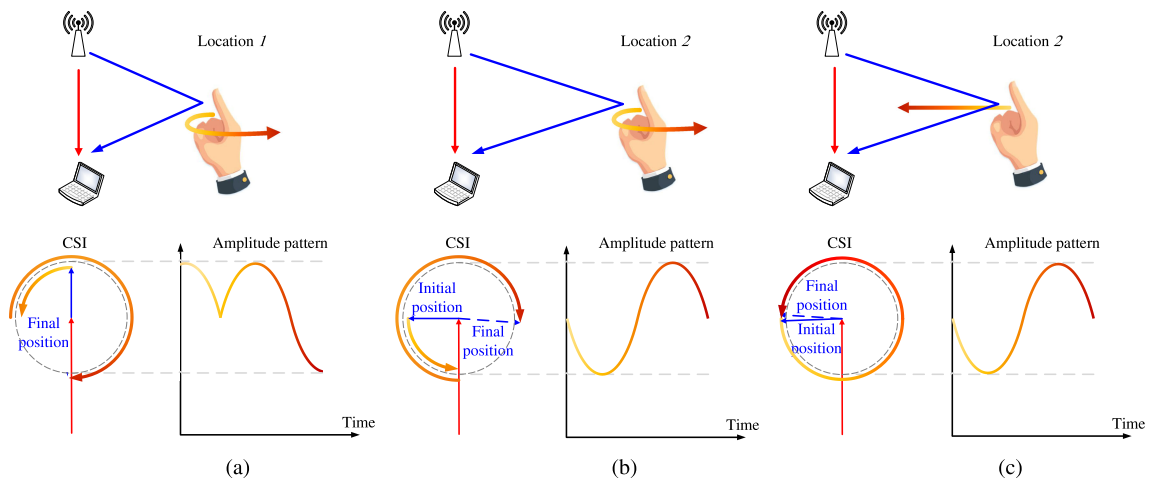


**FIGURE 2.** Illustration of signal pattern inconsistency for recognizing finger gesture with CSI amplitude. Case A and case B are the same gesture performed at different locations, whereas case B and case C are different gestures performed at the same location. (a) Case A. (b) Case B. (c) Case C.

### Limitations of Sensing With Only CSI Amplitude

As elaborated earlier, due to the hardware imperfection, the real-world CSI retrieved from commodity WiFi devices contains noise in amplitude and the phase value is even unusable. Only employing the noisy CSI amplitude for sensing incurs two major issues.

The first limitation is the short sensing range. Contactless WiFi sensing relies on the weak reflection signal that is usually orders of magnitude weaker than the LoS path signal<sup>5</sup> and it becomes even weaker when the target is farther away from the sensing devices. Due to the weak reflection of human body, the target movement-induced signal amplitude variation is easily buried in noise, especially when we tend to track subtle human motions (e.g., millimeter-level chest motion due to respiration), thus resulting in a short sensing range.

The second limitation is the low sensing accuracy. This is due to the signal pattern inconsistency, that is, the targeted human activity location relative to the transceivers has a great impact on the waveform shapes of CSI amplitude.<sup>10,16</sup> To better understand the signal inconsistency, we take the one-dimensional finger gesture recognition as an example, as shown in Figure 2. Three cases are presented in the figure, namely case A, case B, and case C. In each case, we move the finger toward or away from the transceivers, which causes the changes in reflection path length. In case A, the gesture is performed at location 1. We first move the finger toward the transceivers and then move the finger away from the

transceivers. In case B, the same gesture as case A is performed at a different location (location 2). For case C, we only move the finger toward the transceivers at location 2. And in Figure 2, we also present the corresponding CSI change in complex plane and its amplitude variation pattern caused by the finger movement for each case. We can observe that the same gesture performed at different locations results in quite different signal patterns (case A and case B), whereas different gestures performed at the same location result in the same signal pattern (case B and case C). This signal inconsistency would fail most of the widely used learning-based activity recognition approaches,<sup>10</sup> which rely on the assumption that there is a fixed mapping between signal variation patterns and gestures. This is the reason why the existing WiFi-based activity recognition systems cannot achieve high accuracy in real-life applications, where multiple factors can get changed, such as the environment, the location of the WiFi transceivers, and the location of the human target.

## PROPOSED CSI-RATIO MODEL

### Definition of CSI Ratio

MIMO technologies have been widely adopted in modern WiFi devices for data communication, providing multiple transmitting and receiving antennas. Observing the fact that the CSI readings retrieved from different antennas at the same receiver contain very similar hardware noise,<sup>5</sup> we propose to use CSI ratio, which is defined as the quotient of CSI

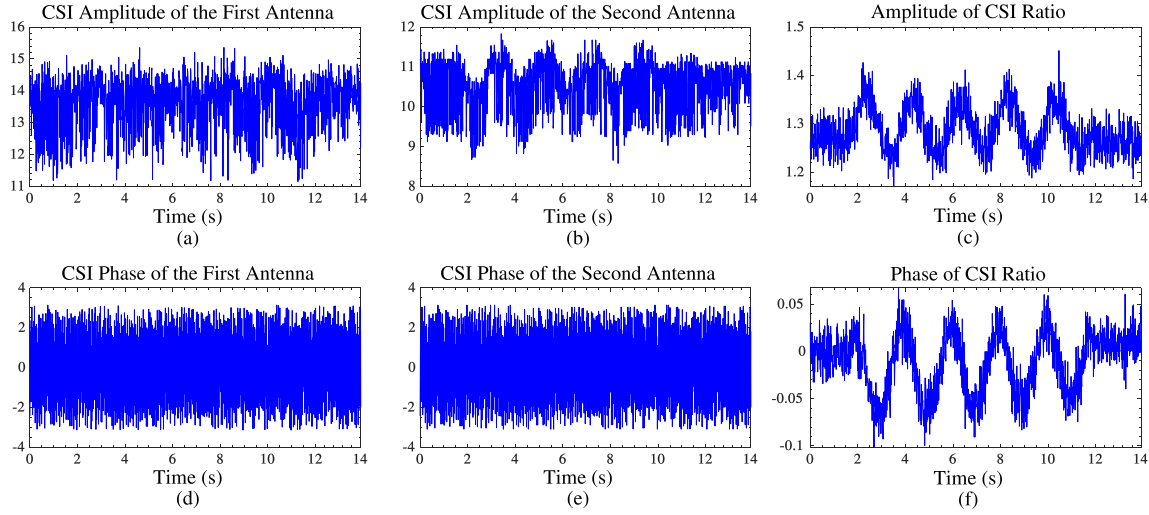


**FIGURE 3.** Comparison of raw CSI and CSI ratio when sensing the plate movement.

readings between two antennas,<sup>5</sup> as a new base signal for sensing

$$H_r(f, t) = \frac{H_1(f, t)}{H_2(f, t)} \quad (4)$$

where  $H_1(f, t)$  is the complex-valued CSI of the first antenna and  $H_2(f, t)$  is that of the second antenna. With multiple available antennas, many CSI ratios can be obtained by employing different pairs of antennas. Each of these CSI ratios can be viewed as an information source, providing us a unique “view” of the observed target. Intuitively, it allows us to combine the information carried by the multiple views to improve the sensing accuracy.

### Noise Cancellation With CSI Ratio

Based on the rule of division operation on two complex numbers, the CSI ratio is still complex-valued, where the resultant amplitude is the quotient of their CSI amplitudes and the phase is the difference between the two CSI phases. For the amplitude, the impulse noise is a scaling one, which amplifies the power at each antenna at the same level on the same receiver.<sup>5,10</sup> In other words, although the power scaling changes over time, it is consistent across different antennas on the same receiver. Thus, the high impulse noise and burst noise that are difficult to remove in the original CSI amplitude can be eliminated by computing the amplitude quotient of two antennas. For the phase, since different antennas on a receiver share the same clock, the phase offsets such as carrier frequency offset and sampling frequency offset are identical.<sup>14,15</sup> Thus, although the phase offsets are

random and time-varying, they are the same across two antennas, which can thus be effectively canceled out by computing the phase difference of two antennas. Thus, (4) can be rewritten as

$$\begin{aligned} H_r(f, t) &= \frac{\delta(t)e^{-j\phi(t)}(H_{s,1}+A_1e^{-j2\pi\frac{d_1(t)}{\lambda}})}{\delta(t)e^{-j\phi(t)}(H_{s,2}+A_2e^{-j2\pi\frac{d_2(t)}{\lambda}})} \\ &= \frac{H_{s,1}+A_1e^{-j2\pi\frac{d_1(t)}{\lambda}}}{H_{s,2}+A_2e^{-j2\pi\frac{d_2(t)}{\lambda}}} \end{aligned} \quad (5)$$

where  $\delta(t)$  is the amplitude impulse noise,  $\phi(t)$  is the time-varying phase offset,  $d_1(t)$  is the target-reflection path length of the first antenna, and  $d_2(t)$  is that of the second antenna. With the division operation, most of the noise in the original CSI amplitude and the time-varying phase offset are successfully canceled out, thus providing a high-SNR base signal for human sensing.

To visualize the effect of noise cancellation with CSI ratio, we conduct a simple experiment with the setup in Figure 1(a). With an LoS length of 5.5 m, we move a metal plate along the perpendicular bisector of the transceivers from 5.83 to 5.99 m. During this process, the reflection path length changes exactly five wavelengths (for 5.24 GHz) and five peaks/valleys are thus expected to appear on the CSI amplitude waveform.<sup>5</sup> Figure 3(a) and (b) shows the raw CSI amplitudes retrieved from two antennas at the same receiver. We can see in Figure 3(a) that the plate movement-induced amplitude variation pattern is buried in the noise. The amplitude variation pattern in Figure 3(b) is slightly clearer. As shown in Figure 3(d) and (e), the raw CSI phases of the two

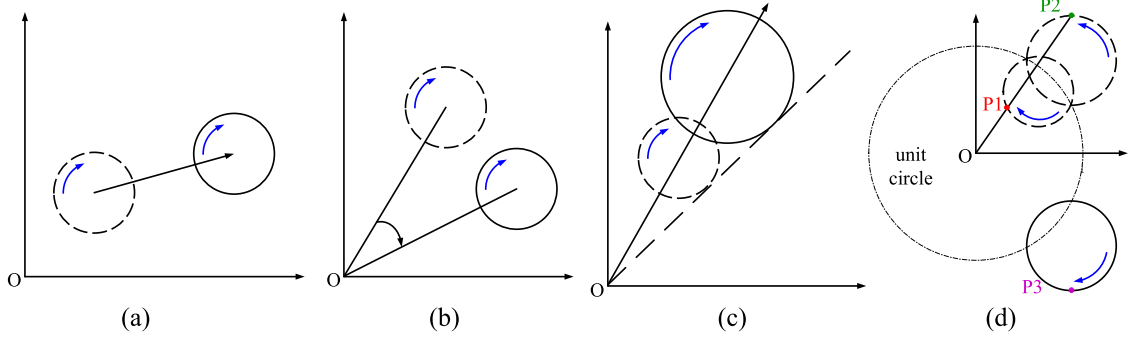


**FIGURE 4.** Möbius transformation can be decomposed into four basic transformations, which preserve the geometric shape of a circle. (a) Translation. (b) Rotation. (c) Scaling. (d) Inversion.

antennas jump randomly, making them unusable. In comparison with the real-world CSI from each individual antenna, Figure 3(c) and (f) shows the amplitude and phase of CSI ratio, respectively. We can clearly observe five peaks/valleys in both amplitude and phase waveforms. Apparently, the CSI ratio of two antennas eliminates noises but retains the signal variation pattern, which can be used for sensing.

### Human Sensing With CSI Ratio

Now let us take a deeper look at how to utilize the CSI ratio for human sensing. To better understand how the target movement affects the CSI ratio, we have an interesting observation to simplify (5): when the target moves a short distance, although the target-reflection path length of each antenna changes, the difference in target-reflection path length between two close-by antennas  $d_2(t) - d_1(t)$  can be seen as a constant. This is because the path length difference changes with the angle of arrival of the signal reflected from the target, which basically remains unchanged.<sup>4,5</sup> With this observation, the CSI ratio in (5) can be rewritten as

$$H_r(f, t) = \frac{A_1 e^{-j2\pi \frac{d_1(t)}{\lambda}} + H_{s,1}}{A_2 e^{-j2\pi \frac{d_2(t)-d_1(t)}{\lambda}} e^{-j2\pi \frac{d_1(t)}{\lambda}} + H_{s,2}} \quad (6)$$

$$= \frac{AZ+B}{CZ+D}$$

where the coefficients  $A, B, C, D$  are complex constants, and  $Z = e^{-j2\pi \frac{d_1(t)}{\lambda}}$  is a unit complex variable, whose phase represents the change in reflection path length.

We observe from (6) that there is only one independent variable  $Z$  left, meaning that the change of CSI ratio solely depends on how the reflection path length changes. Mathematically, (6) is exactly in the form of Möbius transformation (also known as linear

fractional transformation).<sup>17</sup> To study the properties of CSI ratio, we rewrite (6) as

$$H_r(f, t) = \left( \frac{BC-AD}{C^2} \right) \frac{1}{Z+D/C} + \frac{A}{C} \quad (7)$$

$$= \frac{\beta e^{j\theta}}{Z+\alpha} + \gamma$$

where  $\alpha$  and  $\gamma$  are complex numbers and  $\beta$  and  $\theta$  are real numbers. We can see from (7) that the Möbius transformation can be decomposed into four basic transformations, namely translation, rotation, scaling, and inversion. As shown in Figure 4(a)–(c), the translation, rotation, and scaling preserve the geometry shape and rotation direction (clockwise or counterclockwise) of a circle. The inversion preserves the shape of a circle, however, it may change the rotation direction.<sup>5</sup> When the magnitude of static component is larger than that of dynamic component (i.e.,  $|\mathcal{D}| > |\mathcal{C}|$ ), which is the case in human sensing most of time,<sup>5,10</sup> the inversion preserves the rotation direction, as shown in Figure 4(d); otherwise, the inversion changes the rotation direction. Through rigorous mathematical derivation and real-life experiment in<sup>5</sup>, we obtain the following three key properties from the CSI-ratio model in (7) for human sensing.

- 1) The CSI ratio preserves the correlation between target movements and the changes in ideal CSI. Specifically, if the reflection path length changes one wavelength, the CSI ratio would rotate for a full circle in complex plane. And if it changes less than one wavelength, the CSI ratio just rotates for a circular arc.
- 2) If the reflection path length increases: when the magnitude of static component is larger than that of dynamic component, the arc in CSI ratio rotates clockwise; otherwise, it rotates counterclockwise.

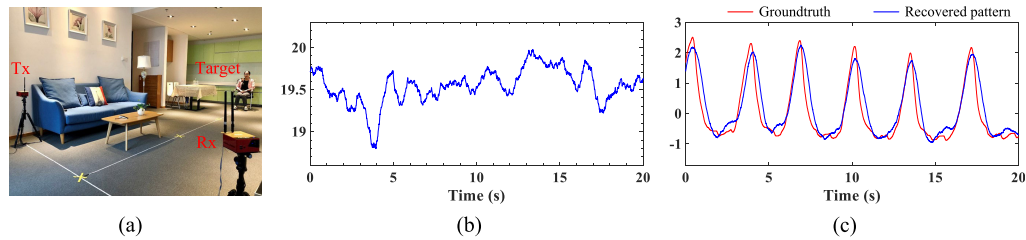


**FIGURE 5.** Comparison with prior work for respiration sensing. (a) Experimental setting. (b) Respiration pattern recovered by prior work that uses CSI amplitude. (c) Respiration pattern recovered by our proposed method that exploits CSI ratio.

- 3) The CSI ratio contains a pair of orthogonal and complementary amplitude/phase information.

### EXPLOITING CSI RATIO TO BOOST WIFI SENSING PERFORMANCE

#### Enlarging Sensing Range

As shown in (5), the amplitude impulse noise and the time-varying phase offset are effectively canceled out by the division operation. Apparently, compared to the raw CSI reading from a single antenna, the CSI ratio between two adjacent antennas contains less noise and is thus more sensitive to detect weak reflected signals, leading to a longer sensing range.

Here, we take human respiration sensing as an example. Prior work<sup>3,6,7</sup> takes the raw CSI amplitude from one antenna to track the millimeter-level chest movement caused by respiration, and they generally have a sensing range of less than 4 m. As a comparison, we take the CSI ratio as the base signal to extract respiration pattern by applying the PCA (Principal Component Analysis) method.<sup>5</sup> We conduct real-world experiments in a home setting, where the target is 8 m away from the transceivers, as shown in Figure 5(a). We collect the ground-truth respiration pattern using a commercial device (Neulog Respiration Monitor Belt logger sensor NUL-236)<sup>5</sup> and present the experimental results in Figure 5(b) and (c). We can see from the figures that the traditional approaches fail to extract clear respiration pattern corresponding to chest movement, whereas the pattern recovered by our proposed approach matches the ground-truth well. With the above experimental setting and a total of 20-h respiration monitoring of three subjects, the mean absolute error of respiration rate is as low as 0.47 bpm (breaths per minute). Extensive experiments in<sup>5</sup> further show that our proposed method is able to robustly detect human respiration through

a 10-cm-thick wall with commodity WiFi, moving one step toward real-life deployment. This case study demonstrates the benefits of applying CSI ratio for respiration sensing.

#### Improving Sensing Accuracy

As previously revealed, the mapping between target movement and CSI amplitude variation is location-dependent, resulting in unstable activity recognition accuracy. Fortunately, the division operation in obtaining CSI ratio cancels out the time-varying phase offset, thus enabling us to utilize the phase information that is unusable with one single antenna. Now that both the complementary amplitude and phase information are available in CSI ratio, we are able to extract a consistent feature corresponding to each activity, which could improve the accuracy in human activity recognition.

We take the finger gesture recognition described in Figure 2 as an example. We show how to utilize the complex-valued CSI ratio to extract a consistent feature that helps to improve the accuracy in recognizing different gestures. We choose the radian change of the arc that the CSI ratio generates in complex plane as the feature. In practice, we track the radian change by measuring the change of the slope for the tangent line at each position on the arc, as shown in Figure 6 (a). Figure 6(b)–(d) presents the radian changes caused by the finger movements corresponding to the three cases in Figure 2. We can observe that the same gesture performed at different locations generates the same feature pattern (case A and case B), whereas different gestures performed at the same location produce different patterns (case B and case C). This is exactly what we want for gesture recognition. To demonstrate the effectiveness of our proposed method, we compare it with the baseline method that directly uses CSI amplitude as the base signal.<sup>16</sup> And we reproduced the experiments in<sup>16</sup> with the same setup in our



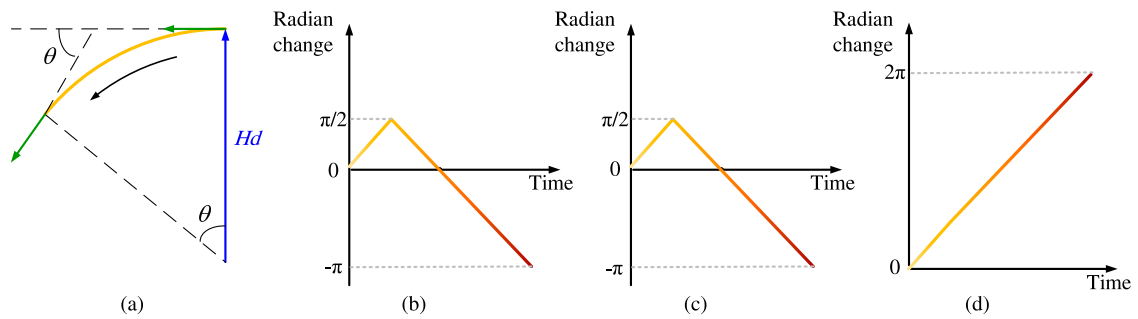


**FIGURE 6.** Radian change of the arc can serve as a consistent feature to distinguish different gestures. (a) Radian change is estimated by measuring the slope change of the tangent line on the arc. (b)–(d) Radian changes in case A, case B, and case C, respectively.

environment. The experimental results demonstrate that, compared to the baseline method, our proposed method increases the sensing accuracy to 97%.

The other example is human respiration monitoring. The existing work<sup>6,7</sup> that utilizes only CSI amplitude faces the “blind-spot” issue, that is, human respiration cannot be effectively detected at certain locations even when the target is close to the sensing devices. In contrast, we elaborately combine the orthogonal amplitude and phase of CSI ratio by the PCA method<sup>5</sup> to extract the respiration pattern. Extensive experiments in<sup>5</sup> show that, by exploiting the CSI ratio, the “blind spots” issue can be fully solved, enabling respiration sensing with a higher accuracy.

## DISCUSSION

### Applying CSI-Ratio Model to Other Sensing Applications and Wireless Signals

The proposed CSI-ratio model is a general-purpose technique, which can be applied not only to fine-grained human activity sensing (e.g., human respiration sensing<sup>5</sup> and finger tracking<sup>10</sup>), but also to coarse-grained human activity sensing (e.g., human tracking<sup>12</sup> and hand gesture recognition<sup>11</sup>). What’s more, the CSI-ratio model is not only applied to OFDM-based WiFi or LTE signals, but also to other wireless signals where the signal readings have both amplitude and phase. For instance, our proposed signal ratio scheme has been successfully applied in LoRa sensing system,<sup>12</sup> which adopts the chirp spread spectrum modulation technique instead of OFDM.

## Multitarget Sensing

In real life, there are scenarios when multiple subjects are in the environment. It is a well-known challenge to separate the signals reflected off multiple targets and achieve multitarget sensing with cheap commodity WiFi hardware. One solution has been proposed in<sup>18</sup> to simultaneously monitor the respiration of multiple persons by leveraging the multiple antennas widely available at commodity WiFi devices. Such an idea may provide researchers a new perspective to recognize activities from multiple targets by exploiting the multiple views provided by many CSI ratios.

## CONCLUSION

In this article, we propose a new base signal called CSI ratio to boost WiFi sensing performance. Two favorable characteristics of CSI ratio are presented and discussed: 1) the CSI ratio cancels out most of the noise in original CSI amplitude and phase, thus providing a high-SNR signal that is very sensitive to human motion; 2) it provides orthogonal and complementary amplitude/phase for sensing, which contains complete information of CSI signal corresponding to human movement. Through two case studies, we demonstrate that these two favorable characteristics can be utilized to significantly enlarge the sensing range and improve the sensing accuracy of many applications. It is worth noting that the proposed CSI ratio can also be applied to other MIMO-based wireless sensing systems, in which the transmitter and receiver are physically separated.

## ACKNOWLEDGMENTS

This work was supported in part by the National Key Research and Development Plan under Grant 2016YFB1001200, in part by the Peking University Information Technology Institute (Tianjin Binhai), and in part by the EU CHIST-ERA Project.

## REFERENCES

1. Y. Ma, G. Zhou, and S. Wang, "WiFi sensing with channel state information: A survey," *ACM Comput. Surv.*, vol. 52, no. 3, 2019, Art. no. 46.
2. W. Wang et al., "Understanding and modeling of WiFi signal based human activity recognition," in *Proc. 21st Annu. Int. Conf. Mobile Comput. Netw.*, 2015, pp. 65–76.
3. D. Zhang, H. Wang, and D. Wu, "Toward centimeterscale human activity sensing with Wi-Fi signals," *IEEE Computer*, vol. 50, no. 1, pp. 48–57, Jan. 2017.
4. Y. Zeng et al., "Fullbreathe: Full human respiration detection exploiting complementarity of CSI phase and amplitude of WiFi signals," *Proc. ACM Interactive, Mobile, Wearable Ubiquitous Technol.*, vol. 2, no. 3, 2018, Art. no. 148.
5. Y. Zeng et al., "FarSense: Pushing the range limit of WiFi-based respiration sensing with CSI ratio of two antennas," *Proc. ACM Interactive, Mobile, Wearable Ubiquitous Technol.*, vol. 3, no. 3, 2019, Art. no. 121.
6. X. Liu, J. Cao, S. Tang, and J. Wen, "Wi-Sleep: Contactless sleep monitoring via WiFi signals," in *Proc. IEEE Real-Time Syst. Symp.*, 2014, pp. 346–355.
7. H. Wang et al., "Human respiration detection with commodity WiFi devices: Do user location and body orientation matter?," in *Proc. ACM Int. Joint Conf. Pervasive Ubiquitous Comput.*, 2016, pp. 25–36.
8. Y. Yang, J. Cao, X. Liu, and X. Liu, "Wi-Count: Passing people counting with COTS WiFi devices," in *Proc. IEEE Int. Conf. Comput. Commun. Netw.*, 2018, pp. 1–9.
9. W. Jiang et al., "Towards environment independent device free human activity recognition," in *Proc. 24th Annu. Int. Conf. Mobile Comput. Netw.*, 2018, pp. 289–304.
10. D. Wu et al., "FingerDraw: Sub-wavelength level finger motion tracking with WiFi signals," *Proc. ACM Interactive, Mobile, Wearable Ubiquitous Technol.*, vol. 4, no. 1, 2020, Art. no. 31.
11. W. Chen et al., "Robust dynamic hand gesture interaction using LTE terminals," in *Proc. IEEE Int. Conf. Inf. Process. Sensor Netw.*, 2020, pp. 109–120.
12. F. Zhang et al., "Exploring LoRa for long-range through-wall sensing," *Proc. ACM Interactive, Mobile, Wearable Ubiquitous Technol.*, vol. 4, no. 2, 2020, Art. no. 27.
13. Y. Zhuo, H. Zhu, H. Xue, and S. Chang, "Perceiving accurate CSI phases with commodity WiFi devices," in *Proc. IEEE Conf. Comput. Commun.*, 2017, pp. 1–9.
14. M. Kotaru et al., "SpotFi: Decimeter level localization using WiFi," *ACM SIGCOMM Comput. Commun. Rev.*, vol. 45, pp. 269–282, 2015.
15. D. Vasisht et al., "Decimeter-level localization with a single WiFi access point," in *Proc. 13th Usenix Conf. Netw. Syst. Des. Implementation*, 2016, pp. 165–178.
16. K. Niu et al., "WiMorse: A contactless Morse code text input system using ambient WiFi signals," *IEEE Internet Things J.*, vol. 6, no. 6, pp. 9993–10008, Dec. 2019.
17. H. Schwerdtfeger, *Geometry of Complex Numbers: Circle Geometry, Moebius Transformation, Non-Euclidean Geometry*. Chelmsford, MA, USA: Courier Corporation, 1979.
18. Y. Zeng et al., "MultiSense: Enabling multi-person respiration sensing with commodity WiFi," *Proc. ACM Interactive, Mobile, Wearable Ubiquitous Technol.*, vol. 4, no. 3, 2020, Art. no. 102.

**YOUWEI ZENG** is currently working toward the Ph.D. degree in computer science in the Key Laboratory of High Confidence Software Technologies (Ministry of Education), School of Electronics Engineering and Computer Science, Peking University, Beijing, China. His research interests include ubiquitous computing and deep learning. He received the B.S. degree in software engineering from Zhejiang University, Hangzhou, China, in 2016. He is the corresponding author of this article. Contact him at ywzeng@pku.edu.cn.

**DAN WU** is currently working toward the Ph.D. degree in computer science in the Key Laboratory of High Confidence Software Technologies (Ministry of Education), School of Electronics Engineering and Computer Science, Peking University, Beijing, China. His research interests include software modeling, mobile sensing, and ubiquitous computing. He received the B.S. degree in computer science from the University of Science and Technology Beijing, Beijing, China. Contact him at dan@pku.edu.cn.



**JIE XIONG** is currently an Assistant Professor in the College of Information and Computer Sciences with the University of Massachusetts Amherst, Amherst, MA, USA. His research interests include wireless sensing and mobile computing. He received the Ph.D. degree in computer science from the University College London, London, U.K., in 2015. He is the recipient of a Google European Doctoral Fellowship and a British Computer Society Distinguished Dissertation Award Runner-Up. His recent work appeared at MobiCom, UbiComp, SenSys, CoNEXT, INFOCOM, NSDI, and won the CoNEXT 2014 Best Paper Award. Contact him at [jxiong@cs.umass.edu](mailto:jxiong@cs.umass.edu).

**DAQING ZHANG** (Fellow, IEEE) is a Chair Professor with the Key Laboratory of High Confidence Software Technologies (Ministry of Education), School of Electronics Engineering and Computer Science, Peking University, Beijing, China, and Telecom SudParis, Evry-Courcouronnes, France. His research

interests include context-aware computing, urban computing, mobile computing, big data analytics, pervasive elderly care, etc. He has authored/coauthored more than 280 technical papers in leading conferences and journals. He received the Ph.D. degree from the University of Rome "La Sapienza," Rome, Italy, in 1996. He was the General or Program Chair for more than 17 international conferences, giving keynote talks at more than 20 international conferences. He is the Associate Editor for the IEEE Pervasive Computing, *ACM Transactions on Intelligent Systems and Technology*, and the Proceedings of ACM on Interactive, Mobile, Wearable and Ubiquitous Technologies. He is the winner of the Ten-Years CoMoRea Impact Paper Award at IEEE PerCom 2013, the Honorable Mention Award at ACM UbiComp 2015 and 2016, the Best Paper Award at IEEE UIC 2015 and 2012. Contact him at [dqzhang@sei.pku.edu.cn](mailto:dqzhang@sei.pku.edu.cn).